University of Groningen

Multi-modal imaging investigation of anterior cingulate cortex cytoarchitecture in neurodevelopment

Forde, Natalie J.; Naaijen, Jilly; Lythgoe, David J.; Akkermans, Sophie E. A.; Openneer, Thaira J. C.; Dietrich, Andrea; Zwiers, Marcel P.; Hoekstra, Pieter J.; Buitelaar, Jan K.

IMPORTANT NOTE: You are advised to consult the publisher's version (publisher's PDF) if you wish to cite from it. Please check the document version below.

Document Version
Publisher's PDF, also known as Version of record

Publication date:
2018

Link to publication in University of Groningen/UMCG research database
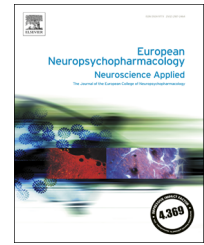
Multi-modal imaging investigation of anterior cingulate cortex cytoarchitecture in neurodevelopment

Natalie J. Forde[a,b,*,1], **Jilly Naaijen**[b,1], **David J. Lythgoe**[c],
Sophie E.A. Akkermans[b], **Thaïra J.C. Openneer**[a],
Andrea Dietrich[a], **Marcel P. Zwiers**[b], **Pieter J. Hoekstra**[a,2],
Jan K. Buitelaar[b,d,2]

[a]*University of Groningen, University Medical Center Groningen, Department of (Child and Adolescent) Psychiatry, Postbus 660, 9700 AR Groningen, The Netherlands*
[b]*Department of Cognitive Neuroscience, Donders Institute for Brain, Cognition and Behavior, Radboud University Medical Center, Nijmegen, The Netherlands*
[c]*King's College London, Institute of Psychiatry, Psychology and Neuroscience, Department of Neuroimaging, London, United Kingdom*
[d]*Karakter Child and Adolescent Psychiatry University Center, Nijmegen, The Netherlands*

Abstract
Multi-modal imaging may improve our understanding of the relationship between cortical morphology and cytoarchitecture. To this end we integrated the analyses of several magnetic resonance imaging (MRI) and spectroscopy (MRS) metrics within the anterior cingulate cortex (ACC). Considering the ACCs role in neurodevelopmental disorders, we also investigated the association between neuropsychiatric symptoms and the various metrics. T1 and diffusion-weighted MRI and ^{1}H-MRS (ACC voxel) data along with phenotypic information were acquired from children (8–12 years) with various neurodevelopmental disorders (n=95) and healthy controls (n=50). From within the MRS voxel mean diffusivity (MD) of the grey matter fraction, intrinsic curvature (IC) of the surface and concentrations of creatine, choline, glutamate, N-acetylaspartate and myo-inositol were extracted. Linear models were used to investigate if the neurochemicals predicted MD and IC or if MD predicted IC. Finally, measures of various

*Corresponding author at: Department of (Child and Adolescent) Psychiatry, University Medical Center Groningen, Postbus 660, 9700 AR Groningen, The Netherlands.
E-mail address:
j.n.forde@umcg.nl (N.J. Forde).
[1]Forde and Naaijen share first authorship.
[2]Hoekstra and Buitelaar share last authorship.

symptom severities were included to determine the influence of symptoms of neurodevelopmental disorders. All five neurochemicals inversely predicted MD (all $p_{uncorrected} < 0.04$, $\beta = 0.23$–0.36). There was no association between IC and MD or IC and the neurochemicals (all $p > 0.05$). Severity of autism symptoms related positively to MD ($p_{uncorrected} = 0.002$, $\beta = 0.39$). Our findings support the notion that the neurochemicals relate to cytoarchitecture within the cortex. Additionally, we showed that autism symptoms across participants relate to the ACC cytoarchitecture.

1. Introduction

Neuroimaging studies continuously falter when it comes to the interpretation of morphological measures. The ability to link morphology with the underlying cytoarchitecture and, even more importantly, with cellular functioning could prove paramount to understanding both healthy functioning and deviations from it that lead to behavioral changes and symptoms seen in neurodevelopmental disorders (Bakhshi and Chance, 2015; Casanova and Trippe, 2009; Kotagiri et al., 2014). Here we have applied a multi-modal approach to determine how several metrics, all purportedly related to the cytoarchitecture albeit measured at different scales, relate to each other. It is likely that one biological process (whether it is deviant or not) is reflected not in just one modality, but to varying extents in several modalities. By using a multi-modal approach the strengths of the different modalities complement each other, providing a more complete picture of the topic under investigation (Curiel et al., 2007).

Many morphological measures of the brain can be derived from T1-weighted magnetic resonance imaging (MRI) data. Intrinsic curvature (IC) is a relatively new morphological index of the cortical surface and it has been proposed to relate to the underlying cell density (Ronan et al., 2011). It is posited that expansion of the surface progresses at different rates across the surface dependent on the cytoarchitecture within the cortex. This process of differential expansion results in changes to the surface, measurable as IC. The degree of differential expansion is less in areas of greater cell density due to the accumulative tangential tension applied by the cells hindering expansion (Ronan et al., 2011; Ronan and Fletcher, 2015). This association suggests IC can be used as a quantifiable measure of the cortical cell density.

Mean diffusivity (MD), an index derived from diffusion-weighted MRI data (dMRI), also relates to the cytoarchitecture. Diffusion-weighted MRI is a technique sensitive to the Brownian movement of water molecules within the tissue. MD is the average amount of diffusion by water in any direction within a voxel. Cell bodies and axons form obstacles to water diffusion, thereby reducing MD. MD therefore will vary dependent on cell density (Beaulieu, 2002), where higher cell density will result in lower MD.

Proton MR Spectroscopy (^{1}H-MRS) allows the non-invasive *in-vivo* quantification of several neurochemicals simultaneously within a selected area of the brain. These include neurochemicals that due to their individual cellular localization can also be used as measures of cell density. For instance, the intracellular concentration of glutamate is several thousand times higher than its extracellular concentration (Danbolt, 2001). Since glutamate is a precursor for GABA and for glutamine in glial cells and a constituent of several types of proteins and peptides (glutathione for example) as well as being a the most common neurotransmitter it is assumed that glutamate is present in every cell of the brain (Hassel and Dingledine, 2012). We are therefore confident that glutamate is related to glutamatergic cell density but also to total cell density. N-Acetylasparate (NAA) has been proposed as a marker of neuronal integrity although its concentration varies across neuronal populations limiting its interpretability (Moffett et al., 2007). Myo-inositol (mI) has been proposed as a glial cell marker (Brand et al., 1993). Choline (Cho) has been proposed as a marker of cellular membrane turnover and cell density (Rae, 2014). Finally, Creatine (Cre) is known as a marker of energy usage but is also highly concentrated in neurons and glia rather than extracellularly and may therefore also act as a proxy for cell density.

Several studies to date used multimodal neuroimaging to investigate associations between different imaging measures and symptoms in different neurodevelopmental disorders. For instance, one study used anatomical MRI, dMRI and ^{1}H-MRS to investigate differences between patients with autism spectrum disorder (ASD) and controls (Libero et al., 2015). Differences between groups were found within all measures in several different brain regions. Similarly, a study investigating bipolar disorder found differences in grey matter (GM) volume, white matter (WM) microstructure and functional connectivity in several regions throughout the brain (Johnston et al., 2017). However, neither study integrated the analyses of the different measures nor did they use the same region of interest across the different measures.

The anterior cingulate cortex (ACC), an important region for cognitive control, attention and emotion regulation (Allman et al., 2001), has been widely implicated in various neurodevelopmental disorders, including Tourette syndrome (TS), obsessive-compulsive disorder (OCD), attention-deficit/hyperactivity disorder (ADHD) and ASD. Studies have reported structural (Ecker et al., 2015; Frodl and Skokauskas, 2012; Kühn et al., 2013; Müller-Vahl et al., 2009; Nakao et al., 2011), neurochemical (Brennan et al., 2013; Freed et al., 2016; Naaijen et al., 2015) and functional (Brennan et al., 2015; Hart et al., 2013; Hull et al., 2017; Neuner et al., 2014; Stern et al., 2000) changes, but findings have been inconsistent. TS, OCD, ADHD and ASD may all show increased

impulsive and compulsive behavior, although to different extents. The ACC has been hypothesized to be involved in regulating these behaviors through top-down cognitive control (Dalley et al., 2011), which makes it an interesting region to investigate across various neurodevelopmental disorders with partially overlapping symptoms.

Here, based on the abovementioned assumptions regarding the relations between the different imaging metrics and cell density, we integrated the analyses of different metrics within the ACC. To this end we used anatomical data, diffusion weighted imaging and ^{1}H-MRS from a cohort of healthy children and children with various neurodevelopmental disorders, including TS, OCD, ADHD and ASD. We hypothesized that the MRS metrics (Glu, NAA and mI concentrations) would be predictive of MD and the degree of IC. Similarly, we expected that MD would predict IC. Which MRS neurochemical best predicts MD and IC may suggest which cellular population has a greater impact on the respective measures. Furthermore, we investigated whether symptoms related to neurodevelopmental disorders were associated with the metrics.

2. Experimental procedures

2.1. Participants

Participants in this study were all reported on previously (Forde et al., 2016; Naaijen et al., 2017, 2016). Briefly, healthy control children were recruited mostly through local schools. Children with neurodevelopmental disorders, including TS, OCD, ADHD and ASD, were recruited via child and adolescent psychiatry/neurology departments and patient associations throughout the Netherlands. Written informed consent was provided by the parents/guardians of all participants and written assent was also given by participants who were 12 years of age. The study was approved by the regional ethics board (CMO Regio Arnhem Nijmegen, numbers: NL42004.091.12 & NL48377.091.14). After quality control of the MRI and MRS data, n=50 healthy controls and n=95 patients (with primary diagnosis of TS, n=40; OCD, n=8; ADHD, n=38; ASD, n=9) were available for statistical analysis. Diffusion MRI data were available for n=36 healthy controls and n=46 patients. See Section 2.6 Quality assessment for details.

Inclusion and exclusion criteria along with information on phenotypic data collection were extensively reported previously (Forde et al., 2016; Naaijen et al., 2017, 2016). Briefly, all participants were 8-12 years old with an IQ>70, were of Caucasian decent, had no contra indications for MR assessment, no previous head injuries or neurological disorders and no major medical illness. Participants of the healthy control group were free of psychiatric disorders as determined by domain scores in the normal range on screening questionnaires (Child behavior checklist [CBCL] and Teacher Report Form [TRF] (Bordin et al., 2013)). A key inclusion criterion for the patient group was meeting DSM-IV criteria for the respective disorders.

2.2. Phenotypic information

TS diagnosis and tic severity were determined and rated using the Yale Global Tic Severity Scale (YGTSS (Leckman et al., 1989)). The Children's Yale-Brown Obsessive Compulsive Scale (CY-BOCS (Scahill et al., 1997)) was used to confirm diagnosis of OCD and determine severity of obsessions and compulsions (in all participants if symptoms were present irrespective of diagnosis). To determine the presence of ADHD and other psychiatric disorders the Kiddie

Schedule for Affective Disorders and Schizophrenia (K-SADS (Kaufman et al., 1997)) interview was administered to the parent(s) of all participants. The screening module was used, followed if needed by disorder-specific modules. ASD was evaluated with the autism diagnostic interview revised (ADI-R; (Lord et al., 1994)), a structured developmental interview to assess ASD symptom severity and classify diagnosis. Information about tic severity was based on the previous week. The K-SADS and the CY-BOCS were conducted about an unmedicated period within the last 6 months, usually the last 48 hours in the case of stimulant medication use.

Phenotypic traits across disorders were further assessed with parental questionnaires including the Conners' Parent Rating Scale – Revised Long version (CPRS-RL (Conners et al., 1997)) to rate total ADHD severity, the Children's Social Behavioral Questionnaire (CSBQ (Luteijn et al., 2000)) to rate core autistic traits, a subscale of the Repetitive Behavior Scale (RBS-R (Lam and Aman, 2007)) to rate repetitive/compulsive behaviors and a medication questionnaire to determine medication history. Full-scale IQ was estimated from four subtests of the Wechsler Intelligence Scale for Children-III (WISC-III (Wechsler, 2002)).

2.3. T1-weighted MRI acquisition

All MRI datasets were acquired on a 3T Siemens Prisma (Siemens, Erlangen, Germany) scanner, located in the Donders Institute for Brain, Cognition and Behavior, Nijmegen, the Netherlands. T1-weighted anatomical images were acquired with a sagittal, 3D magnetization prepared rapid gradient echo (MPRAGE) parallel imaging sequence with the following parameters: TR=2300 ms, TE=2.98 ms, TI=900 ms, FoV=256 mm, slice thickness=1.20 mm, flip angle=9°, in plane resolution=1.0 × 1.0 mm, acceleration factor=2, acquisition time=5:30 min.

2.4. Diffusion-weighted MRI acquisition

Diffusion-weighted datasets were acquired, on a subsample of participants (n=102). After quality control, n=82 remained (n=46 patients and n=36 controls). A pulsed gradient spin-echo echo-planar imaging (EPI) sequence was used. Two non-diffusion weighted reference images (b=0 s/mm^2) and 64 images with a diffusion gradient (b=1500 s/mm^2) were acquired at each of 72 transversal slices with the following parameters: TE=103 ms, TR=12,000 ms, slice thickness=2 mm, in-plane resolution=2 × 2 mm and acquisition time=13:48 min.

2.5. MRS acquisition

Proton spectra were acquired using a point resolved spectroscopy (PRESS) protocol with chemically selective suppression (CHESS) water suppression (Haase et al., 1985). A 2 × 2 × 2 cm voxel was placed on the midline covering pregenual ACC (TR=3000 ms, TE=30 ms, number of averages = 96, bandwidth = 5 kHz, number of points = 4096). Unsuppressed water reference spectra (16 averages) were also acquired. Total acquisition time was six minutes. Voxel location was adjusted for each participant to maximize GM content. See Figure 1A and B for the location of the voxel and an example spectrum. T1-weighted images were used for voxel placement and for tissue segmentation.

2.6. Quality assessment

Anatomical, dMRI and MRS data were all evaluated for data quality. Anatomical and dMRI datasets for each participant were visually inspected (for imaging- and motion artefacts) and evaluated by an experienced rater (NJF) who was blinded to group. Measures of quality such as signal-to-noise ratio (SNR) and motion parameters
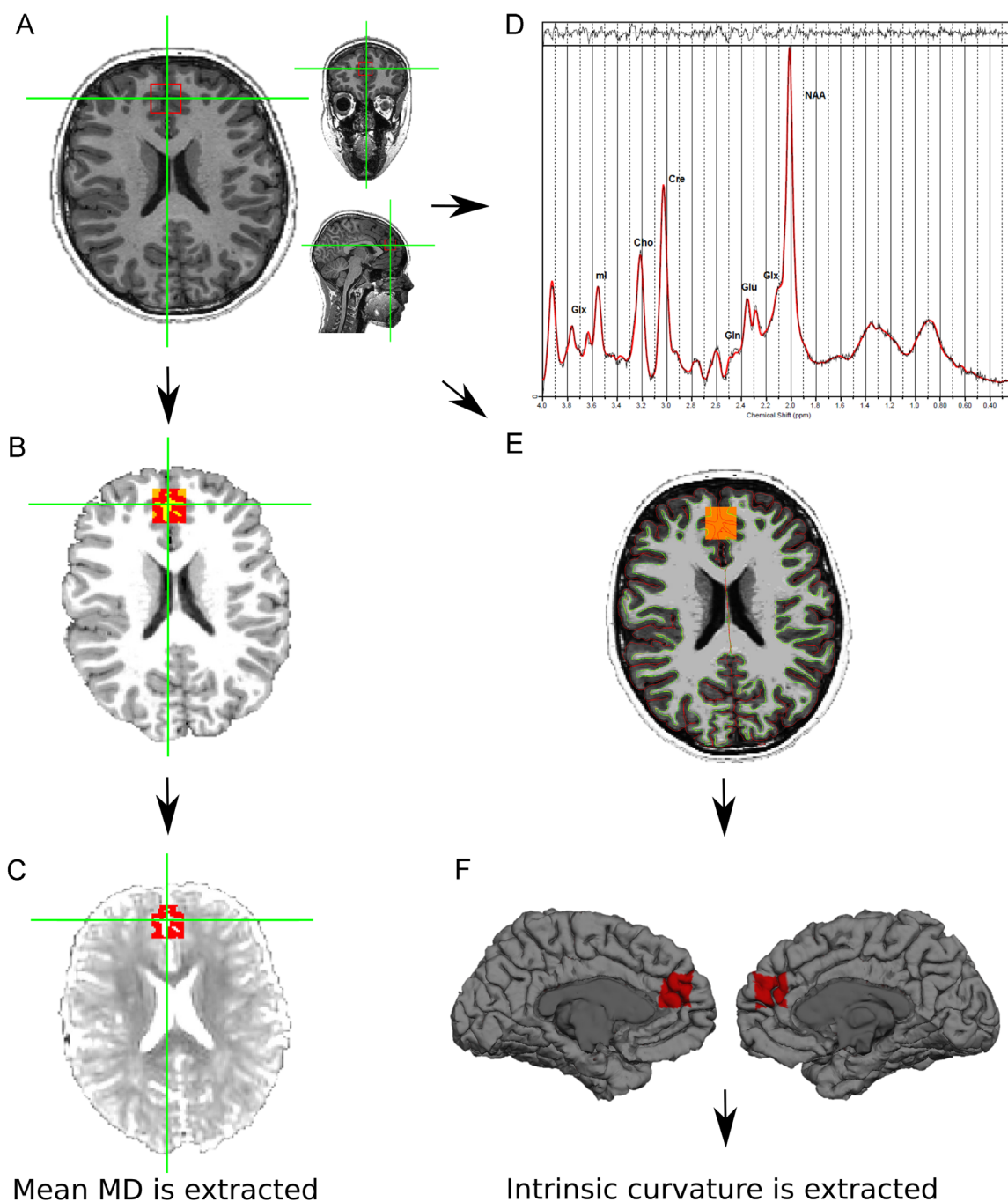
Figure 1 Each processing step for one randomly chosen subject is shown. (A) Localization of the MRS voxel (red) on the T1-weighted image. (B) Skull stripped T1-weighted image with tissue segmented voxel; red, orange and yellow correspond to grey matter, white matter and CSF, respectively. (C) Mean diffusivity (MD) image in T1-weighted space with grey matter fraction of the MRS voxel shown in red. (D) MRS spectrum with peaks corresponding to the major metabolites indicated. The thin black line represents the frequency-domain data, the red line is the LCModel fit. In the top panel the residuals are plotted (the data minus the fit). (E) MRS voxel is shown in orange having been transformed to FreeSurfer space. Green and red lines indicate the white/grey and grey/pial tissue borders, respectively, as defined by FreeSurfer. (F) Red indicates surface within the MRS voxel on the medial pial surface for the left and right hemispheres, respectively. Cho, Choline; Cre, creatine; Gln, glutamine; Glu, glutamate; Glx, Glu+Gln; MD, mean diffusivity; mI, myo-inositol; NAA, N-Acetylaspartate.

were investigated in addition to the visual evaluation. MR spectra were required to have a linewidth (full-width at half-maximum) ≤ 0.1 ppm and SNR ≥ 5 (all spectra were ≥ 19). To ensure similar data quality across the patient and control groups the Cramér-Rao lower bounds (CRLB) were compared for each metabolite of interest

(Kreis, 2015). These did not differ between patients and controls for any of the metabolites (all p-values > 0.1). CRLB estimated standard deviations for Glu, NAA, mI, Cho and Cre for the full sample were 4.3%, 2.1%, 3.3%, 2.4% and 2.0% respectively. Mean voxel percentage GM, WM and cerebrospinal fluid (CSF) were 71.02
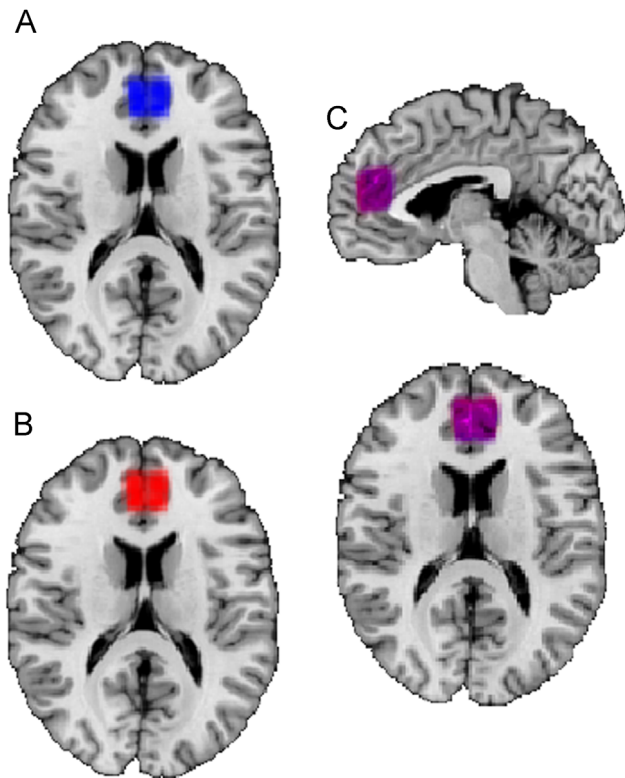
Figure 2 Average voxel placement per group; (A) controls, (B) patients and (C) combined for control and patients groups. Mid-line ACC voxels are superimposed on MNI template. Voxel placement was highly consistent within and across groups.

(6.14) %, 11.42 (2.26) % and 17.53 (6.28) % respectively. These also did not differ between the control and patient groups (all p-values > 0.05; see supplementary Table 2). Consistency of voxel placement across patients and controls can be seen in Figure 2. Chemical shift displacement between mI and NAA was calculated to be approximately 10% of the voxel size as is to be expected from a standard PRESS sequence (Scheenen et al., 2008). Participants with poor quality anatomical/spectral data or with bad anatomical segmentation were excluded from analysis (n=29, these participants were not included in the demographic section/Table I). Twenty additional participants were excluded from analyses of diffusion measures only based on their dMRI quality. Seven additional participants were excluded for having values of more than 3 standard deviations from the mean for our variables of interest. Our final samples for analyses consisted of n=145 (IC and the neurochemicals) and n=82 (analyses including MD).

2.7. Processing

T1-weighted images underwent processing with the unified segmentation procedure within the VBM8 toolbox of SPM8 (Statistical Parametric Mapping 8, UCL, London, UK) to produce GM, WM and CSF probability maps. Spectroscopy voxels were mapped onto these probability maps to generate fractions of GM, WM and CSF within each spectroscopy voxel (f_{GM}, f_{WM} and f_{CSF}).

MRS data were processed with Linear Combination Model (LCModel), version V6.03-0I (Provencher, 2001, 1993), using a linear combination of *in vitro* metabolite solution spectra as a reference to identify and quantify the metabolite concentrations in *in vivo* spectra as described previously (Naaijen et al., 2017, 2016). Briefly, processing included eddy current correction and calculation of water-referenced concentrations in institutional units (i.u.). Each

individual's metabolite concentrations were corrected for partial volume confounds and differing amounts of water in each tissue type with the following formula:

$$\text{Metabolite}_{\text{corrected}} = \text{Metabolite}_{\text{Raw}} * \left(\left(43300 * f_{GM} + 35880 * f_{WM} \right. \right.$$
$$\left. \left. + 55556 * f_{CSF} \right) / 35880 \right) * \left(1 / \left(1 - f_{CSF} \right) \right)$$

where 43,300, 35,880, and 55,556 are the water concentrations in mM for GM, WM, and CSF, respectively. Metabolite$_{\text{corrected}}$ represents the metabolite concentration from the grey and white matter proportion of the MRS voxel, following the LC Model assumption that CSF is free of metabolites (Provencher, 2014).

White and pial cortical surfaces for each hemisphere were reconstructed from the T1-weighted data using the fully automated 'recon-all' procedure in FreeSurfer v5.3 (Dale et al., 1999; Fischl et al., 1999a, 1999b; Fischl et al., 1999a, 1999b; Fischl and Dale, 2000). These cortical reconstructions were used in the Caret software (v5.65, http://brainvis.wustl.edu/wiki/index.php/Caret:About) to calculate the IC per vertex as described previously (Forde et al., 2014; Ronan et al., 2014). Diffusion-weighted data were de-noised with a local principal component analysis (LPCA) noise filter as well as affine transformed to correct for motion and eddy current distortions (SPM8, London, UK). Susceptibility distortions were non-linearly corrected along the phase encoding direction to optimally match the T1-weighted image (Visser et al., 2010). Finally, diffusion tensors were robustly estimated using the PATCH (Zwiers, 2010) algorithm to eliminate artifacts in the data from cardiac and head motion.

2.8. Extracting metrics from within the MRS voxel

A transformation matrix was generated by registering (fslregister) the T1-weighted image in native space to the FreeSurfer anatomical image. This transformation was then applied to the binarized MRS voxel file while converting it to a surface (mri_vol2surf), which resulted in a surface file that masked the region within the MRS voxel for each hemisphere in FreeSurfer space.

The IC files for each hemisphere were imported to Matlab (R2012b) where IC values from the region within the MRS voxel were isolated using the surface masks previously generated. These were then filtered to remove IC values inconsistent with the resolution of reconstruction (Ronan et al., 2014, 2012) before calculating the absolute values of the remaining per-vertex IC measures. Values for left and right were combined before the skewness of the IC distribution for the region within the MRS voxel was computed (Ronan et al., 2014, 2012). The distribution of cortical IC values is highly skewed towards zero (Pienaar et al., 2008; Ronan et al., 2012, 2011). Therefore, it is more informative to use the dimensionless measure of skew, rather than mean or median, as a measure of the degree of differential expansion in the region. We infer that the less skewed the distribution the greater the degree of IC, which is proposed to reflect a lower cell density.

A transformation matrix from diffusion to T1-weighted space was generated by linearly registering the average $b=0$ s/mm^2 image to the T1-weighted image using FMRIB's Linear Image Registration Tool (FLIRT) (Jenkinson et al., 2002; Jenkinson and Smith, 2001). This matrix was then applied to the MD image to transform it to T1 space. The GM fraction of the MRS voxel was isolated and binarized with fslmaths. Fslstats was then used to extract metrics from the MD image from within the GM masked region (Smith et al., 2004; Woolrich et al., 2009).

2.9. Statistics

Statistical analyses were conducted with the R statistical program (R Core Team, 2013). Pearson's chi-squared tests were used to examine the differences between the control and patient groups in categorical measures (sex and handedness). Group differences in continuous measures (age and IQ) were assessed with a Welch two
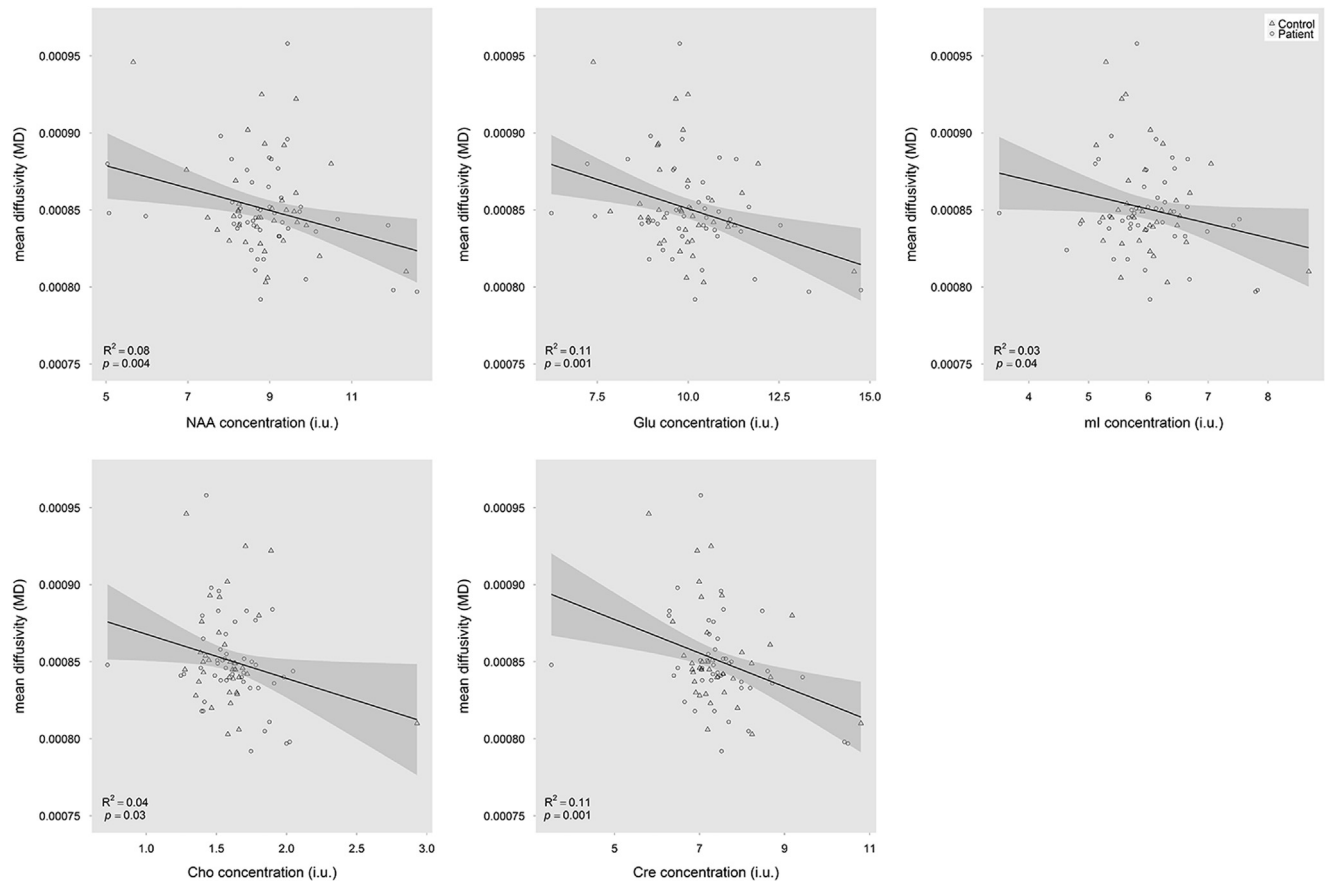
Figure 3 Figures show the raw data points and regression fit lines with their 95% confidence intervals (shaded areas) for association between the neurochemicals and mean diffusivity (MD). R^2 and p-values are derived from the linear models including age and sex. A similar pattern of negative association is seen between all neurochemicals and MD (Note: statistical analyses indicate positive t-stats due to the Box-Cox transformations). Cho – choline, Cre – creatine, Glu – glutamate, mI – myo-Inositol, NAA – N-Acetylaspartate, i.u. - institutional units.

sample t-test if assumptions of homogeneity of variance and normality of distributions were met ($p > 0.05$ in Bartlett test of homogeneity of variance and Shapiro-Wilk normality test). If either of these assumptions were violated a non-parametric Mann-Whitney U test was used. Group differences in voxel tissue composition and spectral quality were assessed with Welch two sample t-test (if normal and homogenous, as above).

To address our primary question, i.e. are the MRS metrics, MD and IC associated, we used linear models including age and sex to determine if the respective metabolites (NAA, Glu, mI, Cho and Cre) predicted IC skew and MD (subset of data) and if MD predicted IC skew. When residuals of the model were not normally distributed we used a Box-Cox power transformation (Box and Cox, 1964) to normalize the data. As our variables of interest were not totally independent, corrections for multiple comparisons (eleven tests) were based on the effective number of tests (Nyholt, 2004). This resulted in an adjusted alpha level of 0.006 (based on 8.2 effective tests rather than eleven). Subsequently, we added phenotypic data to the models to address our second question; do cross-disorder symptoms of neurodevelopmental disorders significantly relate to the metrics? Here, ADHD severity (T-score) (CPRS; Conners et al. 1998), ASD core symptoms (CSBQ; Luteijn et al. 2000), repetitive and compulsive behaviors (RBS-R; Lam and Aman 2007), TS (yes/no) (YGTSS; Leckman et al. 1989) and IQ were examined in addition to sex and age.

As a visual aid to understand the shared variance of the MR metrics we also conducted a principal component analysis (PCA) including participants for whom data for each metric were available

(n=82). The principle components were not further analyzed, as the above methods were deemed more suitable to address our specific research question and to make better use of the available data. The principle components are not specific to the metrics nor do they give information on how related each metric is to another. Results from the PCA analysis can be found in Supplementary Table 3 and Supplementary Figure 1.

3. Results

3.1. Demographics

Participant demographic details are reported in Table I (n=145). The patient group included participants with a primary diagnosis of TS, n=40; OCD, n=8; ADHD, n=38; ASD, n=9. For more detailed demographic information regarding the patient group and comorbidities, see Supplementary Table SI. For the analyses including MD, the number of participants was fewer (n=46 and n=36 for patients and controls, respectively). This reduction did not affect the demographic distributions between groups (n=82; age, t=-1.36, p=0.18; sex, χ^2=0.50, p=0.48; IQ, t=-3.11, p=0.003; handedness, $\chi^2 < 0.01$, p=0.99).

Participants in the patient group frequently had multiple comorbid conditions (see Supplementary Table SI) as is common in neurodevelopmental disorders (Anholt et al., 2010; Huisman-van Dijk et al., 2016). Furthermore, there was a sex imbalance across the different disorders, most notably in the TS group where there were considerably more male than female participants. This is consistent with population estimates of neurodevelopmental disorders (Hirschtritt et al., 2015).

3.2. Neurochemicals predicting MD

In our basic models (including age and sex) we saw that all tested neurochemicals predicted MD (NAA: $\beta=0.32$, $t=2.94$, $p=0.004$; Glu: $\beta=0.36$, $t=3.36$, $p=0.001$; mI: $\beta=0.23$, $t=2.05$, $p=0.04$; Cho: $\beta=0.24$, $t=2.21$, $p=0.03$; Cre: $\beta=0.36$, $t=3.40$, $p=0.001$), although mI and Cho failed to reach statistical significance following multiple comparison correction (adjusted alpha = 0.006). In each case there was a negative association between MD and the neurochemical (statistical analyses show a positive t-stat due to Box-Cox transformations), see Figure 3.

These findings were negligibly influenced by the inclusion of phenotypic data. None of the phenotypic information had a significant effect on the models (all p-values >0.02). However, autism symptoms (CSBQ core score) and compulsive behaviors (RBS compulsivity subscale) consistently appeared to affect the models although not significantly considering the adjusted alpha level (0.006) (CSBQ: $p=0.02$-0.03; RBS $p=0.04$-0.06). We further investigated each of these phenotypic measures with respect to NAA, Glu, mI, Cho, Cre and MD individually using a linear model. This showed that autism

Figure 4 Figures show the raw data points and regression fit line with its 95% confidence interval (shaded area) for the association between the Children's Social Behavior Checklist (CSBQ; Luteijn et al. 2000) core autism symptoms and mean diffusivity (MD). R^2 and p-values are derived from the linear model including age and sex.

traits significantly predicted MD ($\beta=0.39$, $t=3.29$, $p=0.002$, see Figure 4) but not any of the metabolite concentrations (all p-values >0.2). Compulsive behaviors did not significantly predict MD or any of the neurochemical concentrations ($p>0.07$).

3.3. Neurochemicals predicting IC

None of the neurochemicals significantly predicted IC skew (NAA: $\beta=-0.15$, $t=-1.75$, $p=0.08$; Glu: $\beta=0.05$, $t=0.62$, $p=0.54$; mI: $\beta=0.10$, $t=1.17$, $p=0.25$; Cho: $\beta=0.08$, $t=0.94$, $p=0.35$; Cre: $\beta=0.10$, $t=1.20$, $p=0.23$). The inclusion of phenotypic data did not significantly influence the model (all p-values >0.05).

3.4. MD predicting IC

MD did not predict IC skew ($\beta=-0.05$, $t=-0.43$, $p=0.67$). However, sex had a significant main effect ($\beta=0.28$, $t=2.56$, $p=0.01$).

To ensure our findings were not unduly affected by the inclusion of patients, we repeated our analyses regarding whether the respective measures were associated with each other in the healthy control group only (n=50 or n=36 when MD was investigated). As expected due to the decrease in power associated with reducing subject number none of our findings of neurochemicals predicting MD remained significant, however, the pattern and size of effects remained stable (NAA: $\beta=0.32$, $t=1.88$, $p=0.07$; Glu: $\beta=0.34$, $t=2.02$, $p=0.05$; mI: $\beta=0.26$, $t=1.51$, $p=0.14$; Cho: $\beta=020$, $t=1.13$, $p=0.27$; Cre: $\beta=0.35$, $t=2.11$, $p=0.04$). Results involving IC skew were also similar to those of the full group.

4. Discussion

In the current study we investigated whether there was an association between several different structural and neurochemical metrics, which are all theoretically related to cell density, within the ACC. As hypothesized, concentrations of all five neurochemicals investigated (NAA, Glu, mI, Cho and Cre) were related to MD, although mI and Cho concentration was not significantly related to MD after correction for multiple comparisons. In each case there was a negative association between MD and the neurochemical concentration (statistical analyses show a positive t-stat due to Box-Cox transformations). This supports the notion that water diffusion (quantified by MD) is hindered by cells (both neuronal and glial) and varies with cell density. Opposed to our hypothesis we saw no association between neurochemical concentrations or MD with the degree of IC of the surface. Finally, we investigated whether symptoms related to neurodevelopmental disorders, including autism symptom severity, attention, hyperactivity, compulsivity, obsessions and tics, were associated with the metrics. We showed a negative association between autism symptom severity and MD within the ACC region investigated. This suggests higher cell density in the ACC is associated with more severe autism symptoms across disorders.

We proposed that Glu concentration could be used as a proxy for cell density. The current finding of a negative

correlation between Glu and MD supports this idea. As mentioned above, diffusion of water molecules (quantified by MD) is hindered by cells, thus with a higher cell density MD is lower. A previous study in a male group of healthy adults found a similar association between Glu concentration and MD, albeit in a different region of interest – posterior cingulate cortex (PCC) (Arrubla et al., 2017). Another previous study reported a negative association between NAA and MD in the centrum semiovale WM of controls and patients with cerebrovascular disease (Nitkunan et al., 2008) which they interpreted as relating to axonal loss or dysfunction. Our findings are in line with those of both studies and additionally show similar associations between MD and mI/Cho/Cre that have not previously been reported to the best of the authors' knowledge. However, the associations here for mI and Cho were not significant following multiple comparison correction and warrant replication.

There was no significant relationship between IC skew and neurochemical concentrations or between IC skew and MD indicating that IC does not directly relate to the underlying cortical cell density. This is not to say that during development of the cortical cell density does not influence differential surface expansion and thereby IC and cortical folding as hypothesized (Ronan et al., 2011; Ronan and Fletcher, 2015). The only thing we can infer from our results is that at the age of our participants (8-12 years) the relationship is not present. This may be due to several other factors. For instance the cortex at this age is no longer expanding but is in fact reducing in thickness (Amlien et al., 2016; Brown et al., 2012; Ostby et al., 2009; Raznahan et al., 2011; Shaw et al., 2008), surface area (according to some sources (Brown et al., 2012; Ostby et al., 2009; Raznahan et al., 2011; Shaw et al., 2012)) and gyrification (Raznahan et al., 2011; Shaw et al., 2012). These processes may obscure any relationship that would once have been present. As well as this differential expansion leads to cortical folding which itself is thought to alter the cortical cell density in places which would in turn effect future surface expansion and result in a complex association of IC to cell density (Ronan and Fletcher, 2015).

Severity of autism symptoms across disorders was inversely related to MD. From this we infer that those with more severe autistic traits have a higher cell density (which restricts water diffusion and results in a lower MD). This is in line with a former study of the same cohort where increased Glu concentrations were found in participants with ASD compared to controls in the same region of interest (Naaijen et al., 2016). Additionally, in this previous study Glu concentration in the ACC was positively correlated with a measure of repetitive behavior (limited interest) across ASD and OCD patients, supporting the assumption of higher cell density across disorders with an increase in autism symptom severity. Another former study has shown increased Cho and mI in ASD compared to controls in the ACC which is in accordance with the current finding of an inverse relationship with MD (Vasconcelos et al., 2008). Previous research has suggested cytoarchitectural changes in ASD (Casanova and Trippe, 2009). A study in adults with ASD showed atypical intrinsic cortico-cortical connectivity compared with controls at the level of grey matter, indicating cytoarchitectural abnormalities (Ecker et al., 2013). In another study of adults with ASD lower cell density was shown in the septal hypocellular gap of the subventricular zone, however, comparing this to the current study is difficult as a sub-cortical region was investigated and layer specific abnormalities were found (Kotagiri et al., 2014). Several of these studies refer to a strong genetic component involved in cytoarchitectural changes. It would therefore be worthwhile to investigate genetic factors underlying these cytoarchitectural changes along with the neurochemicals and MD in future studies.

Strengths of the current study were the investigation of a relatively large group of children with a restricted age range (8–12 years). Although investigating a heterogeneous group of participants with several different neurodevelopmental disorders can have limitations, by utilizing dimensional measures across the groups we could address our research questions better than would have otherwise been possible. This dimensional approach has been advocated by Robbins and colleagues (Robbins et al., 2012) and the research domain criteria (RDoC) initiative (Cuthbert, 2014) as opposed to categorizing participants based on arbitrary thresholds. Furthermore, to account for the possible confound of heterogeneity caused by the different diagnostic groups, we performed an internal replication in the healthy controls, which showed similar results, although non-significant due to reduced power. A further strength of the current study was the use of several metrics, all with a theoretical relationship to cell density, in one region of interest. These metrics complement each other to give more information than investigating them individually.

In conclusion, the current study showed that the concentrations of various neurochemicals are inversely associated with MD supporting the notion that they all relate to cell density within the cortex. IC on the other hand was unrelated to the other metrics investigated suggesting that it is not directly related to the cell density within the cortex. Finally, our findings support evidence that autism symptoms across disorders relate to the cytoarchitecture in the ACC. Whether this extends to other areas needs further examination.

Role of funding source

Contributors

Buitelaar designed the study and wrote the protocol. Forde and Naaijen managed the literature searches. Forde, Naaijen, Zwiers and Lythgoe conducted the analyses. Statistical analyses were undertaken by Forde and Naaijen, who also wrote the initial draft of the manuscript. All authors reviewed, contributed and approved the final manuscript.

Conflict of interest

D.J. Lythgoe has acted as a consultant for Ixico PLC. P.J. Hoekstra has been a member of the advisory board of Shire. J.K. Buitelaar has been in the past 3 years a consultant to / member of advisory board of / and/or speaker for Janssen Cilag BV, Eli Lilly, Shire,

Appendix A.   Supporting information

Supplementary data associated with this article can be found in the online version at https://doi.org/10.1016/j. euroneuro.2017.11.021.

References

Allman, J.M., Hakeem, a, Erwin, J.M., Nimchinsky, E., Hof, P., 2001. The anterior cingulate cortex. The evolution of an interface between emotion and cognition. Ann. N. Y. Acad. Sci 935, 107–117. http://dx.doi.org/10.1111/j.1749-6632.2001.tb03476.x.

Amlien, I.K., Fjell, A.M., Tamnes, C.K., Grydeland, H., Krogsrud, S. K., Chaplin, T.A., Rosa, M.G.P., Walhovd, K.B., 2016. Organizing principles of human cortical development—thickness and area from 4 to 30 Years: insights from comparative primate neuroanatomy. Cereb. Cortex 26, 257–267. http://dx.doi.org/10.1093/cercor/bhu214.

Anholt, G.E., Cath, D.C., Van Oppen, P., Eikelenboom, M., Smit, J.H., Van Megen, H., Van Balkom, A.J.L.M., 2010. Autism and adhd symptoms in patients with ocd: are they associated with specific oc symptom dimensions or oc symptom severity. J. Autism Dev. Disord. 40, 580–589. http://dx.doi.org/10.1007/s10803-009-0922-1.

Arrubla, J., Farrher, E., Strippelmann, J., Tse, D.H.Y., Grinberg, F., Shah, N.J., Neuner, I., 2017. Microstructural and functional correlates of glutamate concentration in the posterior cingulate cortex. J. Neurosci. Res. 0. http://dx.doi.org/10.1002/jnr.24010.

Bakhshi, K., Chance, S.A., 2015. The neuropathology of schizophrenia: a selective review of past studies and emerging themes in brain structure and cytoarchitecture. Neuroscience 303, 82–102. http://dx.doi.org/10.1016/j.neuroscience.2015.06.028.

Beaulieu, C., 2002. The basis of anisotropic water diffusion in the nervous system – a technical review. NMR Biomed. 15, 435–455. http://dx.doi.org/10.1002/nbm.782.

Bordin, I. a, Rocha, M.M., Paula, C.S., Teixeira, M.C.T.V., Achenbach, T.M., Rescorla, L. a, Silvares, E.F.M., 2013. Child Behavior Checklist (CBCL),Youth Self-Report (YSR) and Teacher's Report Form(TRF): an overview of the development of the original and Brazilian versions. Cad. Saude Publica 29, 13–28. http://dx.doi.org/10.1590/S0102-311X2013000500004.

Box, G.E.P., Cox, D.R., 1964. An analysis of transformations. J. R. Stat. Soc. 26, 211–252.

Brand, A., Richter-Landsberg, C., Leibfritz, D., 1993. Multinuclear NMR studies on the energy metabolism of glial and neuronal cells. Dev. Neurosci. 15, 289–298.

Brennan, B.P., Rauch, S.L., Jensen, J.E., Pope, H.G., 2013. A critical review of magnetic resonance spectroscopy studies of obsessive-compulsive disorder. Biol. Psychiatry 73, 24–31. http://dx.doi.org/10.1016/j.biopsych.2012.06.023.

Brennan, B.P., Tkachenko, O., Schwab, Z.J., Juelich, R.J., Ryan, E. M., Athey, A.J., Pope, H.G., Jenike, M. a, Baker, J.T., Killgore, W. D., Hudson, J.I., Jensen, J.E., Rauch, S.L., 2015. An examination of rostral anterior cingulate cortex function and neurochemistry in obsessive-compulsive disorder. Neuropsychopharmacology 40, 1–11. http://dx.doi.org/10.1038/npp.2015.36.

Brown, T.T., Kuperman, J.M., Chung, Y., Erhart, M., McCabe, C., Hagler, D.J., Venkatraman, V.K., Akshoomoff, N., Amaral, D.G., Bloss, C.S., Casey, B.J., Chang, L., Ernst, T.M., Frazier, J.A., Gruen, J.R., Kaufmann, W.E., Kenet, T., Kennedy, D.N., Murray, S.S., Sowell, E.R., Jernigan, T.L., Dale, A.M., 2012. Neuroanatomical assessment of biological maturity. Curr. Biol. 22, 1693–1698. http://dx.doi.org/10.1016/j.cub.2012.07.002.

Casanova, M., Trippe, J., 2009. Radial cytoarchitecture and patterns of cortical connectivity in autism. Philos. Trans. R. Soc. Lond. B. Biol. Sci. 364, 1433–1436. http://dx.doi.org/10.1098/rstb.2008.0331.

Conners, C.K., Sitarenios, G., Parker, J.D., Epstein, J.N., 1998. The revised Conners' Parent Rating Scale (CPRS-R): factor structure, reliability, and criterion validity. J. Abnorm. Child Psychol. 26, 257–268.

Conners, C.K., Wells, K.C., Parker, J.D., Sitarenios, G., Diamond, J. M., Powell, J.W., 1997. A new self-report scale for assessment of adolescent psychopathology: factor structure, reliability, validity, and diagnostic sensitivity. J. Abnorm. Child Psychol. 25, 487–497.

Curiel, L., Chopra, R., Hynynen, K., 2007. Progress in multimodality imaging: truly simultaneous ultrasound and magnetic resonance imaging. IEEE Trans. Med. Imaging 26, 1740–1747. http://dx.doi.org/10.1109/TMI.2007.903572.

Cuthbert, B.N., 2014. The RDoC framework: facilitating transition from ICD/DSM to dimensional approaches that integrate neuroscience and psychopathology. World Psychiatry 13, 28–35. http://dx.doi.org/10.1002/wps.20087.

Dale, A.M., Fischl, B., Sereno, M.I., 1999. Cortical surface-based analysis. I. Segmentation and surface reconstruction. Neuroimage 9, 179–194. http://dx.doi.org/10.1006/nimg.1998.0395.

Dalley, J.W., Everitt, B.J., Robbins, T.W., 2011. Impulsivity, compulsivity, and top-down cognitive control. Neuron 69, 680–694. http://dx.doi.org/10.1016/j.neuron.2011.01.020.

Danbolt, N.C., 2001. Glutamate uptake. Prog. Neurobiol. 65, 1–105. http://dx.doi.org/10.1016/S0301-0082(00)00067-8.

Ecker, C., Bookheimer, S.Y., Murphy, D.G.M., 2015. Neuroimaging in autism spectrum disorder: brain structure and function across the lifespan. Lancet Neurol. 14, 1121–1134. http://dx.doi.org/10.1016/S1474-4422(15)00050-2.

Ecker, C., Ronan, L., Feng, Y., Daly, E., Murphy, C., Ginestet, C.E., Brammer, M., Fletcher, P.C., Bullmore, E.T., Suckling, J., Baron-Cohen, S., Williams, S., Loth, E., Murphy, D.G.M., 2013. Intrinsic gray-matter connectivity of the brain in adults with autism spectrum disorder. Proc. Natl. Acad. Sci. USA 110, 13222–13227. http://dx.doi.org/10.1073/pnas.1221880110.

Fischl, B., Dale, A.M., 2000. Measuring the thickness of the human cerebral cortex from magnetic resonance images. Proc. Natl. Acad. Sci. USA 97, 11050–11055. http://dx.doi.org/10.1073/pnas.200033797.

Fischl, B., Sereno, M.I., Dale, A.M., 1999a. Cortical surface-based analysis. II: inflation, flattening, and a surface-based coordinate system. Neuroimage 9, 195–207. http://dx.doi.org/10.1006/nimg.1998.0396.

Fischl, B., Sereno, M.I., Tootell, R.B., Dale, A.M., 1999b. High-resolution intersubject averaging and a coordinate system for the cortical surface. Hum. Brain Mapp. 8, 272–284. http://dx.doi.org/10.1002/(SICI)1097-0193(1999)8:4<272::AID-HBM10>3.0.CO;2-4.

Forde, N.J., Ronan, L., Suckling, J., Scanlon, C., Neary, S., Holleran, L., Leemans, A., Tait, R., Rua, C., Fletcher, P.C.,

Jeurissen, C., Dodds, C.M., Miller, S.R., Bullmore, E.T., McDonald, C., Nathan, P.J., Cannon, D.M., 2014. Structural neuroimaging correlates of allelic variation of the BDNF val66met polymorphism. Neuroimage 90, 280-289. http://dx.doi.org/10.1016/j.neuroimage.2013.12.050.

Forde, N.J., Zwiers, M.P., Naaijen, J., Akkermans, S.E.A., Openneer, T.J.C., Visscher, F., Dietrich, A., Buitelaar, J.K., Hoekstra, P.J., 2016. Basal ganglia structure in Tourette's disorder and/or attention-deficit/hyperactivity disorder. Mov. Disord. 0, 1-5. http://dx.doi.org/10.1002/mds.26849.

Freed, R.D., Coffey, B.J., Mao, X., Weiduschat, N., Kang, G., Shungu, D.C., Gabbay, V., 2016. Decreased anterior cingulate cortex γ-aminobutyric acid in youth with tourette's disorder. Pediatr. Neurol. 65, 64-70. http://dx.doi.org/10.1016/j.pediatrneurol.2016.08.017.

Frodl, T., Skokauskas, N., 2012. Meta-analysis of structural MRI studies in children and adults with attention deficit hyperactivity disorder indicates treatment effects. Acta Psychiatr. Scand. 125, 114-126. http://dx.doi.org/10.1111/j.1600-0447.2011.01786.x.

Haase, A., Frahm, J., Hänicke, W., Matthaei, D., 1985. 1H NMR chemical shift selective (CHESS) imaging. Phys. Med. Biol. 30, 341-344. http://dx.doi.org/10.1088/0031-9155/30/4/008.

Hart, H., Radua, J., Nakao, T., Mataix-Cols, D., Rubia, K., 2013. Meta-analysis of functional magnetic resonance imaging studies of inhibition and attention in attention-deficit/hyperactivity disorder: exploring task-specific, stimulant medication, and age effects. JAMA Psychiatry 70, 185-198. http://dx.doi.org/10.1001/jamapsychiatry.2013.277.

Hassel, B., Dingledine, R., 2012. Glutamate and Glutamate Receptors, In: Basic Neurochemistry. pp. 342-366.

Hirschtritt, M.E., Lee, P.C., Pauls, D.L., Dion, Y., Grados, M. a, Illmann, C., King, R. a, Sandor, P., McMahon, W.M., Lyon, G.J., Cath, D.C., Kurlan, R., Robertson, M.M., Osiecki, L., Scharf, J.M., Mathews, C. a, 2015. Lifetime prevalence, age of risk, and genetic relationships of comorbid psychiatric disorders in Tourette syndrome. JAMA Psychiatry 72, 325. http://dx.doi.org/10.1001/jamapsychiatry.2014.2650.

Huisman-van Dijk, H.M., Schoot, R. van de, Rijkeboer, M.M., Mathews, C.A., Cath, D.C., 2016. The relationship between tics, OC, ADHD and autism symptoms: a cross- disorder symptom analysis in Gilles de la Tourette syndrome patients and family-members. Psychiatry Res. 237, 138-146. http://dx.doi.org/10.1016/j.psychres.2016.01.051.

Hull, J.V., Jacokes, Z.J., Torgerson, C.M., Irimia, A., Van Horn, J.D., 2017. Resting-state functional connectivity in autism spectrum disorders: a review. Front. Psychiatry 7, 205. http://dx.doi.org/10.3389/FPSYT.2016.00205.

Jenkinson, M., Bannister, P., Brady, M., Smith, S., 2002. Improved optimization for the robust and accurate linear registration and motion correction of brain images. Neuroimage 17, 825-841. http://dx.doi.org/10.1016/S1053-8119(02)91132-8.

Jenkinson, M., Smith, S., 2001. A global optimisation method for robust affine registration of brain images. Med. Image Anal. 5, 143-156. http://dx.doi.org/10.1016/S1361-8415(01)00036-6.

Johnston, J.A.Y., Wang, F., Liu, J., Blond, B.N., Wallace, A., Liu, J., Spencer, L., Cox Lippard, E.T., Purves, K.L., Landeros-Weisenberger, A., Hermes, E., Pittman, B., Zhang, S., King, R., Martin, A., Oquendo, M.A., Blumberg, H.P., 2017. Multimodal neuroimaging of frontolimbic structure and function associated with suicide attempts in adolescents and young adults with bipolar disorder. Am. J. Psychiatry AJP 2016 (1). http://dx.doi.org/10.1176/appi.ajp.2016.15050652.

Kaufman, J., Birmaher, B., Brent, D., Rao, U., Flynn, C., Moreci, P., Williamson, D., Ryan, N., 1997. Schedule for affective disorders and schizophrenia for school-age children-present and lifetime version (K-SADS-PL): initial reliability and validity data. J. Am. Acad. Child Adolesc. Psychiatry 36, 980-988. http://dx.doi.org/10.1097/00004583-199707000-00021.

Kotagiri, P., Chance, S.A., Szele, F.G., Esiri, M.M., 2014. Subventricular zone cytoarchitecture changes in Autism. Dev. Neurobiol. 74, 25-41. http://dx.doi.org/10.1002/dneu.22127.

Kreis, R., 2015. The trouble with quality filtering based on relative Cramér-Rao lower bounds. Magn. Reson. Med. 18, 15-18. http://dx.doi.org/10.1002/mrm.25568.

Kühn, S., Kaufmann, C., Simon, D., Endrass, T., Gallinat, J., Kathmann, N., 2013. Reduced thickness of anterior cingulate cortex in obsessive-compulsive disorder. Cortex 49, 2178-2185. http://dx.doi.org/10.1016/j.cortex.2012.09.001.

Lam, K.S.L., Aman, M.G., 2007. The repetitive behavior scale-revised: independent validation in individuals with autism spectrum disorders. J. Autism Dev. Disord. 37, 855-866. http://dx.doi.org/10.1007/s10803-006-0213-z.

Leckman, J.F., Riddle, M.A., Hardin, M.T., Ort, S.I., Swartz, K.L., Stevenson, J., Cohen, D.J., 1989. The Yale Global Tic Severity Scale: initial testing of a clinician-rated scale of tic severity. J. Am. Acad. Child Adolesc. Psychiatry 28, 566-573. http://dx.doi.org/10.1097/00004583-198907000-00015.

Libero, L.E., DeRamus, T.P., Lahti, A.C., Deshpande, G., Kana, R.K., 2015. Multimodal neuroimaging based classification of autism spectrum disorder using anatomical, neurochemical, and white matter correlates. Cortex 66, 46-59. http://dx.doi.org/10.1016/j.cortex.2015.02.008.

Lord, C., Rutter, M., Couteur, A.L., 1994. Autism Diagnostic Interview - Revised: a revised version of a diagnostic interview for caregivers of individuals with possible pevasive developmental disorders. J. Autism Dev. Disord. 24, 659-685. http://dx.doi.org/10.1007/BF02172145.

Luteijn, E., Luteijn, F., Jackson, S., Volkmar, F., Minderaa, R., 2000. The Children's Social Behavior Questionnaire for milder variants of PDD problems: evaluation of the psychometric characteristics. J. Autism Dev. Disord. 30, 317-330. http://dx.doi.org/10.1023/A:1005527300247.

Moffett, J.R., Ross, B., Arun, P., Madhavarao, C.N., Namboodiri, A.M.A., 2007. N-Acetylaspartate in the CNS: from neurodiagnostics to neurobiology. Prog. Neurobiol. 81, 89-131. http://dx.doi.org/10.1016/j.pneurobio.2006.12.003.

Müller-Vahl, K.R., Kaufmann, J., Grosskreutz, J., Dengler, R., Emrich, H.M., Peschel, T., 2009. Prefrontal and anterior cingulate cortex abnormalities in Tourette Syndrome: evidence from voxel-based morphometry and magnetization transfer imaging. BMC Neurosci. 10, 47. http://dx.doi.org/10.1186/1471-2202-10-47.

Naaijen, J., Forde, N.J., Lythgoe, D.J., Akkermans, S.E.A., Openneer, T.J.C., Dietrich, A., Zwiers, M.P., Hoekstra, P.J., Buitelaar, J.K., 2017. Fronto-striatal glutamate in children with Tourette's disorder and attention-deficit/hyperactivity disorder. NeuroImage Clin. 13, 16-23. http://dx.doi.org/10.1016/j.nicl.2016.11.013.

Naaijen, J., Lythgoe, D.J., Amiri, H., Buitelaar, J.K., Glennon, J.C., 2015. Fronto-striatal glutamatergic compounds in compulsive and impulsive syndromes: a review of magnetic resonance spectroscopy studies. Neurosci. Biobehav. Rev. 52, 74-88. http://dx.doi.org/10.1016/j.neubiorev.2015.02.009.

Naaijen, J., Zwiers, M.P., Amiri, H., Williams, S.C.R., Durston, S., Oranje, B., Brandeis, D., Boecker-Schlier, R., Ruf, M., Wolf, I., Banaschewski, T., Glennon, J.C., Franke, B., Buitelaar, J.K., Lythgoe, D.J., 2016. Fronto-striatal glutamate in autism spectrum disorder and obsessive compulsive disorder. Neuropsychopharmacology, 1-35. http://dx.doi.org/10.1038/npp.2016.260.

Nakao, T., Radua, J., Rubia, K., Mataix-Cols, D., 2011. Gray matter volume abnormalities in ADHD: voxel-based meta-analysis exploring the effects of age and stimulant medication. Am. J. Psychiatry 168, 1154-1163. http://dx.doi.org/10.1176/appi.ajp.2011.11020281.

Neuner, I., Werner, C.J., Arrubla, J., Stöcker, T., Ehlen, C., Wegener, H.P., Schneider, F., Shah, N.J., 2014. Imaging the where and when of tic generation and resting state networks in adult Tourette patients. Front. Hum. Neurosci. 8, 362. http://dx.doi.org/10.3389/fnhum.2014.00362.

Nitkunan, A., Charlton, R.A., McIntyre, D.J.O., Barrick, T.R., Howe, F.A., Markus, H.S., 2008. Diffusion tensor imaging and MR spectroscopy in hypertension and presumed cerebral small vessel disease. Magn. Reson. Med. 59, 528-534. http://dx.doi.org/10.1002/mrm.21461.

Nyholt, D.R., 2004. A simple correction for multiple testing for single-nucleotide polymorphisms in linkage disequilibrium with each other. Am. J. Hum. Genet. 74, 765-769. http://dx.doi.org/10.1086/383251.

Ostby, Y., Tamnes, C.K., Fjell, A.M., Westlye, L.T., Due-Tønnessen, P., Walhovd, K.B., 2009. Heterogeneity in subcortical brain development: a structural magnetic resonance imaging study of brain maturation from 8 to 30 years. J. Neurosci. 29, 11772-11782. http://dx.doi.org/10.1523/JNEUROSCI.1242-09.2009.

Pienaar, R., Fischl, B., Caviness, V., Makris, N., Grant, P.E., 2008. A methodology for analyzing curvature in the developing brain from preterm to adult. Int. J. Imaging Syst. Technol. 18, 42-68. http://dx.doi.org/10.1002/ima.20138.

Provencher, S., 2014. LCModel & LCMgui User's Manual.

Provencher, S.W., 1993. Estimation of metabolite concentrations from localized in vivo proton NMR spectra. Magn. Reson. Med. 30, 672-679. http://dx.doi.org/10.1002/mrm.1910300604.

Provencher, S.W., 2001. Automatic quantitation of localized in vivo 1H spectra with LCModel. NMR Biomed. 14, 260-264. http://dx.doi.org/10.1002/nbm.698.

R Core Team, 2013. R: A language and environment for Statistical computing.

Rae, C.D., 2014. A guide to the metabolic pathways and function of metabolites observed in human brain 1H magnetic resonance spectra. Neurochem. Res. 39, 1-36. http://dx.doi.org/10.1007/s11064-013-1199-5.

Raznahan, A., Shaw, P., Lalonde, F., Stockman, M., Wallace, G.L., Greenstein, D., Clasen, L., Gogtay, N., Giedd, J.N., 2011. How does your cortex grow? J. Neurosci. 31, 7174-7177. http://dx.doi.org/10.1523/JNEUROSCI.0054-11.2011.

Robbins, T.W., Gillan, C.M., Smith, D.G., de Wit, S., Ersche, K.D., 2012. Neurocognitive endophenotypes of impulsivity and compulsivity: towards dimensional psychiatry. Trends Cogn. Sci. 16, 81-91. http://dx.doi.org/10.1016/j.tics.2011.11.009.

Ronan, L., Fletcher, P.C., 2015. From genes to folds: a review of cortical gyrification theory. Brain Struct. Funct. 220, 2475-2483. http://dx.doi.org/10.1007/s00429-014-0961-z.

Ronan, L., Pienaar, R., Williams, G., Bullmore, E., Crow, T.J., Roberts, N., Jones, P.B., Suckling, J., Fletcher, P.C., 2011. Intrinsic curvature: a marker of millimeter-scale tangential cortico-cortical connectivity? Int. J. Neural Syst. 21, 351-366. http://dx.doi.org/10.1142/S0129065711002948.

Ronan, L., Voets, N., Rua, C., Alexander-Bloch, A., Hough, M., Mackay, C., Crow, T.J., James, A., Giedd, J.N., Fletcher, P.C., 2014. Differential tangential expansion as a mechanism for cortical gyrification. Cereb. Cortex 24, 2219-2228. http://dx.doi.org/10.1093/cercor/bht082.

Ronan, L., Voets, N.L., Hough, M., Mackay, C., Roberts, N., Suckling, J., Bullmore, E., James, A., Fletcher, P.C., 2012.

Consistency and interpretation of changes in millimeter-scale cortical intrinsic curvature across three independent datasets in schizophrenia. Neuroimage 63, 611-621. http://dx.doi.org/10.1016/j.neuroimage.2012.06.034.

Scahill, L., Riddle, M.A., McSwiggin-Hardin, M., Ort, S.I., King, R.A., Goodman, W.K., Cicchetti, D., Leckman, J.F., 1997. Children's Yale-Brown Obsessive Compulsive Scale: reliability and validity. J. Am. Acad. Child Adolesc. Psychiatry 36, 844-852. http://dx.doi.org/10.1097/00004583-199706000-00023.

Scheenen, T.W.J., Klomp, D.W.J., Wijnen, J.P., Heerschap, A., 2008. Short echo time 1H-MRSI of the human brain at 3T with minimal chemical shift displacement errors using adiabatic refocusing pulses. Magn. Reson. Med. 59, 1-6. http://dx.doi.org/10.1002/mrm.21302.

Shaw, P., Kabani, N.J., Lerch, J.P., Eckstrand, K., Lenroot, R., Gogtay, N., Greenstein, D., Clasen, L., Evans, A., Rapoport, J.L., Giedd, J.N., Wise, S.P., 2008. Neurodevelopmental trajectories of the human cerebral cortex. J. Neurosci. 28, 3586-3594. http://dx.doi.org/10.1523/JNEUROSCI.5309-07.2008.

Shaw, P., Malek, M., Watson, B., Sharp, W., Evans, A., Greenstein, D., 2012. Development of cortical surface area and gyrification in attention-deficit/hyperactivity disorder. Biol. Psychiatry 72, 191-197. http://dx.doi.org/10.1016/j.biopsych.2012.01.031.

Smith, S.M., Jenkinson, M., Woolrich, M.W., Beckmann, C.F., Behrens, T.E.J., Johansen-Berg, H., Bannister, P.R., De Luca, M., Drobnjak, I., Flitney, D.E., Niazy, R.K., Saunders, J., Vickers, J., Zhang, Y., De Stefano, N., Brady, J.M., Matthews, P.M., 2004. Advances in functional and structural MR image analysis and implementation as FSL. Neuroimage 23, S208-S219. http://dx.doi.org/10.1016/j.neuroimage.2004.07.051.

Stern, E., Silbersweig, D.A., Chee, K.Y., Holmes, A., Robertson, M.M., Trimble, M., Frith, C.D., Frackowiak, R.S., Dolan, R.J., 2000. A functional neuroanatomy of tics in Tourette syndrome. Arch. Gen. Psychiatry 57, 741-748. http://dx.doi.org/10.1001/archpsyc.57.8.741.

Vasconcelos, M.M., Brito, A.R., Domingues, R.C., Da Cruz, L.C.H., Gasparetto, E.L., Werner, J., Gonçalves, J.P.S., 2008. Proton magnetic resonance spectroscopy in school-aged autistic children. J. Neuroimaging 18, 288-295. http://dx.doi.org/10.1111/j.1552-6569.2007.00200.x.

Visser, E., Quin, S., Zwiers, M., 2010. EPI distortion correction by constrained nonlinear coregistration improves group MRI, In: ISMRM. Stockholm, Sweden.

Wechsler, D., 2002. WISC-III Handleiding. The Psychological Corporation, London.

Woolrich, M.W., Jbabdi, S., Patenaude, B., Chappell, M., Makni, S., Behrens, T., Beckmann, C., Jenkinson, M., Smith, S.M., 2009. Bayesian analysis of neuroimaging data in FSL. Neuroimage 45, S173-S186. http://dx.doi.org/10.1016/j.neuroimage.2008.10.055.

Zwiers, M.P., 2010. Patching cardiac and head motion artefacts in diffusion-weighted images. Neuroimage 53, 565-575, http://dx.doi.org/10.1016/j.neuroimage.2010.06.014.